Chapter 9

# Mass Transfer in Multiphase Systems

Badie I. Morsi and Omar M. Basha

Additional information is available at the end of the chapter

http://dx.doi.org/10.5772/60516

**Abstract**

Mass transfer in reactive and non-reactive multiphase systems is of vital importance in chemical, petrochemical, and biological engineering applications. In this chapter, theories and models of mass transfer in gas-liquid, gas-solid and gas-liquid-solid systems with and without chemical reactions are briefly reviewed. Literature data on the mass transfer characteristics in multiphase reactors over the last two decades with applications to the Fischer-Tropsch (F-T) synthesis are summarized. Moreover, the F-T reactions are described and an overview of the use of Slurry Bubble Column Reactors (SBCRs) and Multitubular Fixed Bed Reactors (MTFBRs) for low temperature F-T (LTFT) synthesis are discussed. The important factors affecting the hydrodynamic (gas holdup, bubble size/distribution) and mass transfer parameters (volumetric mass transfer coefficients) in SBCRs for F-T synthesis, including operating conditions, gas-liquid-solid properties, reactor geometry and internals as well as gas distributors are also discussed. The discussion reveals that the performance of the LTFT SBCR operating in the churn-turbulent flow regime is controlled by the resistance in the liquid-side film and/or the F-T reaction kinetics depending on the operating conditions prevailing in the reactor. Also, there is a great need to understand the behavior and quantify the hydrodynamics and mass transfer in SBCRs operating with syngas ($H_2$ + CO) and F-T reactor wax in the presence of active catalyst (iron or cobalt) under typical F-T synthesis conditions in a large SBCR with an inside diameter ≥0.15m.

**Keywords:** Mass Transfer, Multiphase Systems, Fischer Tropsch, Slurry Bubble Column

## 1. Introduction

Mass transfer in multiphase (gas-liquid-solid) systems is one of the most critical processes occurring in chemical, petrochemical, and biological engineering applications. Generally, it entails transport of species among phases through diffusion (physical) and/or chemical reactions in a special unit operation (reactor), allowing such a process to take place. Chemical reactions, often used to speed up the mass transfer rate, occur whenever species of different chemical potentials are brought into contact. In multiphase systems, the species mass transfer rate is controlled not only by the system pressure and temperature, but also by the conductance of mass transfer, concentration gradients, reaction kinetics, activation energy, etc. In some cases, either the conductance of mass transfer or the reaction kinetics could control the overall mass transfer rate; and the slowest one will be the rate limiting or controlling step. For instance, oxygen transfer from the feed (gas) to the aqueous solution (liquid) in bioreactors could be the overall rate limiting step [1]. In any case, understanding mass transfer behavior in multiphase systems requires, among others, precise knowledge of all aspects affecting the overall mass transfer rate [2].

## 2. Mass transfer theories

There are different theories dealing with mass transfer among phases, such as the two-film theory, the penetration theory and the surface renewal theory. These theories are briefly discussed below.

### 2.1. Two-film theory

This is the oldest theory for gas-liquid mass transfer developed by Lewis and Whitman in 1924 [3]. The theory postulates the existence of a film of a thickness (δ) in both the gas and liquid phases separated by an interface. It is based on the following assumptions: (1) the mass transfer occurs by molecular diffusion through the film, beyond which the concentration ($C_{Ab}$) is homogeneous; (2) the mass transfer through the film occurs under steady state conditions; and (3) the flux is small and the mass transfer occurs at low concentration. Accordingly, for convective mass transfer, the concentration profile is linear as shown in Figure 1 and the liquid-side mass transfer coefficient is expressed by Equation (1):

$$k_L = \frac{D_{AB}}{\delta_L} \tag{1}$$

One should remember that the actual concentration profile is nonlinear as can be seen in Figure 1. In turbulent flow, however, attempts were made to relate the mass transfer coefficient with the turbulent diffusivity, which obviously is different from that in the laminar flow. Surprisingly, some experimental results were modeled with limited success using this simplistic model, where $k_L$ values were found to be proportional to the diffusivity to the power one. However, one should keep in mind that the film theory does not provide a direct means for estimating the film thickness.

http://dx.doi.org/10.5772/60516

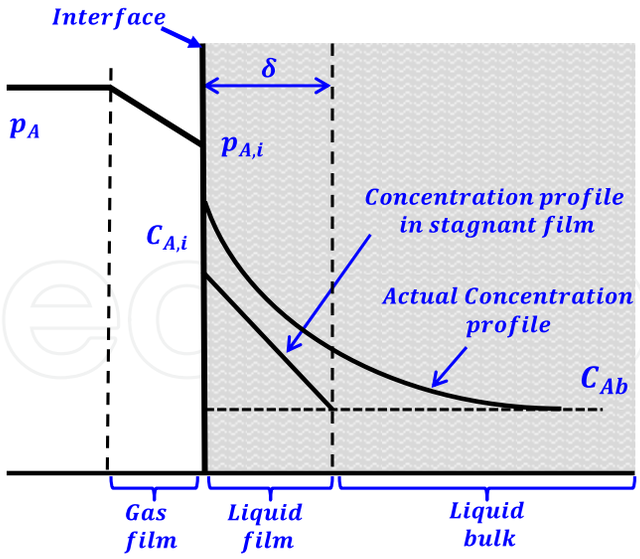


**Figure 1.** Schematic of two film theory

## 2.2. Penetration theory

The "penetration theory" or "Higbie's model" [4] assumes that each liquid element at the gas-liquid interface is exposed to the gas for a short time, as schematically shown in Figure 2. The basic assumptions of the theory are: (1) mass transfer from the gas into a liquid element occurs under unsteady-state conditions once they are in contact; (2) each of the liquid elements stays in contact with the gas for same time period; and (3) equilibrium exists at the gas-liquid interface. This theory was considered an improvement from the two-film theory since mass transfer occurs under unsteady-state conditions in many industrial processes. The penetration theory expresses the liquid-side mass transfer coefficient in terms of the contact time ($\theta$) and the molecular diffusivity of the gas in the liquid according to Equation (2).

$$k_L = 2\left(\frac{D_{AB}}{\pi\theta}\right)^{0.5} \tag{2}$$

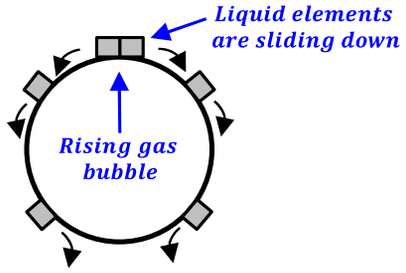


**Figure 2.** Schematic of Higbie's model

### 2.3. Surface renewal theory

The surface renewal theory, developed by Danckwerts [5], applies mathematics of the penetration theory to a more plausible situation, where the liquid is pictured as two regions, a large well mixed bulk region and an interfacial region, which is renewed so fast that it behaves as a thick film as shown in Figure 3. The basic assumptions of the theory are (1) liquid elements at the interface are being randomly swapped by fresh elements from the bulk; (2) at any moment, each of the liquid elements at the interface has the same probability of being substituted by a fresh element; and (3) mass transfer from the gas into the liquid element during its stay at the interface takes place under unsteady-state conditions. Thus, instead of using a constant contact time ($\theta$), the differential liquid volume at the gas-liquid interface is renewed due to the turbulence around the interface, referred to as the surface renewal frequency ($s$). The surface renewal theory expresses the liquid-side mass transfer coefficient in terms of the surface renewal frequency ($s$) and the molecular diffusivity of the gas in the liquid according to Equation (3).

$$k_L = \left(D_{AB} s\right)^{0.5} \tag{3}$$

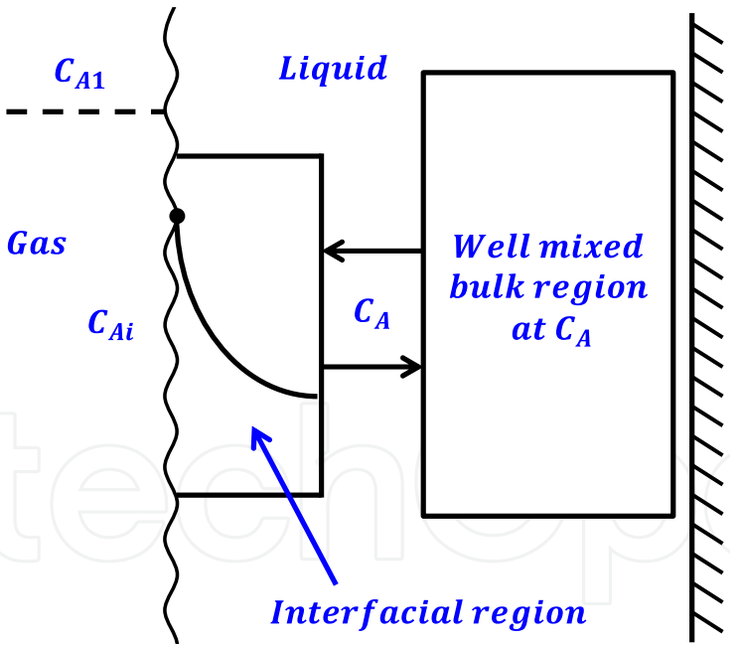


**Figure 3.** Schematic of surface renewal theory

In all three theories, $D_{AB}$ is the molecular diffusivity of the gas (solute A) into the liquid (solvent B) at infinite dilution (up to 5 mol% of the solute in the solvent). However, one should keep in mind that the diffusivity depends to a large extent on the temperature, solvent viscosity as well as on the solvent composition and nature. A number of investigators related $k_L$ to $D_{AB}$ in the form $k_L \alpha (D_{AB})^{m}$ as given in Table 1.

| Author | Variable | Diffusivity Exponent |
|---|---|---|
| Versteeg et al. [6] | $k_L$ | 0.33-0.5 |
| Davies et al. [7] | $k_L$ | 0.46-0.60 |
| Kuthan and Broz [8] | $k_L$ | 0.51-0.64 |
| Kozinski and King [9] | $k_L$ | 0.5-0.6 |
| Linek et al. [10] | $k_L$ | 0.46-0.66 |

**Table 1.** $k_L$ relationship with diffusivity

## 3. Mass transfer with chemical reaction

### 3.1. Gas-liquid systems

In the absence of chemical reactions, the gas (A) diffuses into a liquid (B) and the mass transfer rate can be expressed using the following diffusivity equation:

$$\frac{\partial c_A}{\partial t} = -D_{AB}\frac{\partial^2 c_A}{\partial x^2} \tag{4}$$

The steady-state mass transfer flux through the liquid film can be described according to the film theory by Equation (5).

$$J_i = k_{L,i}a(C_i^* - C_{i,L}) \tag{5}$$

Where $C_i^*$ represents the solute concentration at the gas-liquid interface, $C_{i,L}$ is the solute concentration in the liquid bulk, $k_L$ is the liquid-side mass transfer coefficient, and $a$ represents the gas-liquid interfacial area.

In the presence of chemical reactions, the film theory was also used to interpret gas-liquid mass transfer, however, modifications were required since the actual concentration profiles are no longer linear as can also be seen in Figure 4. This is due to the fact that chemical reactions could vary from slow to extremely fast, whereby instantaneous reactions occur at the interface; fast reactions occur in a narrow zone within the liquid film, and slow reactions spread through the film as well as the liquid bulk. Thus, in order to account for the effect of the chemical reaction on the solute mass transfer, an enhancement factor ($E$), defined as the ratio of the absorption rate with and without the reaction, is introduced as follows:

$$E = \frac{Mass\ transfer\ rate\ with\ chemical\ reaction}{Mass\ transfer\ rate\ without\ chemical\ reaction} \tag{6}$$

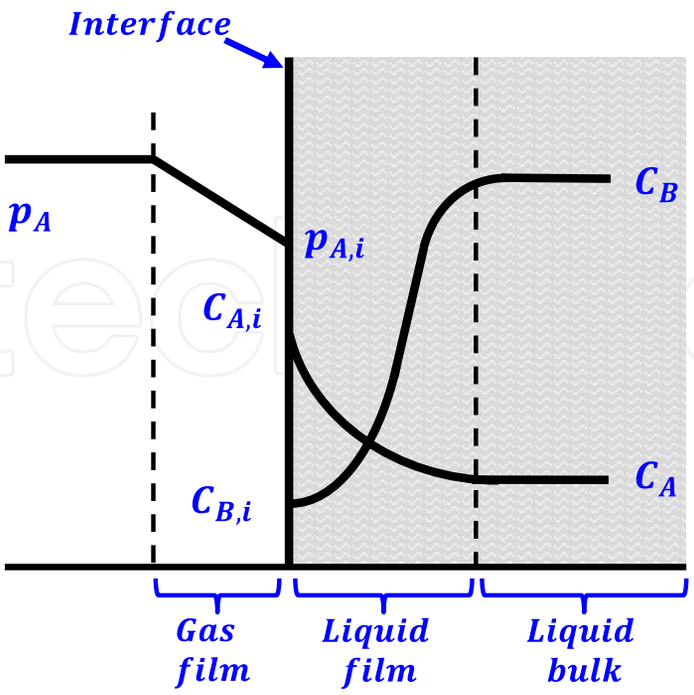


**Figure 4.** Mass transfer with chemical reaction in a gas-liquid system

An irreversible m[th], n[th] orders chemical reaction can be expressed by the following equation:

$$mA + nB \rightarrow P(product) \tag{7}$$

The reaction rate can be written as:

$$-r_A = k_{m,n} C_A^m C_B^n \tag{8}$$

The enhancement factor has been extensively investigated with many approximations proposed for solving Equation (8). The most widely used approximation is the numerical solution proposed by van Krevelen and Hoftijzer [11], which estimates the value of the enhancement factor as a function of the Hatta number (Ha). Ha compares the rate of chemical reaction to that of diffusion through the film and the enhancement factor for an infinitely fast reaction ($E_\infty$), is shown in Figure 5. For a chemical reaction expressed by Equation (8), Ha could be written as:

$$Ha = \frac{\sqrt{\frac{2}{(m+1)} k_{m,n} C_{A,i}^{m-1} C_{B,bulk}^n D_{A,B}}}{k_L} \tag{9}$$

http://dx.doi.org/10.5772/60516

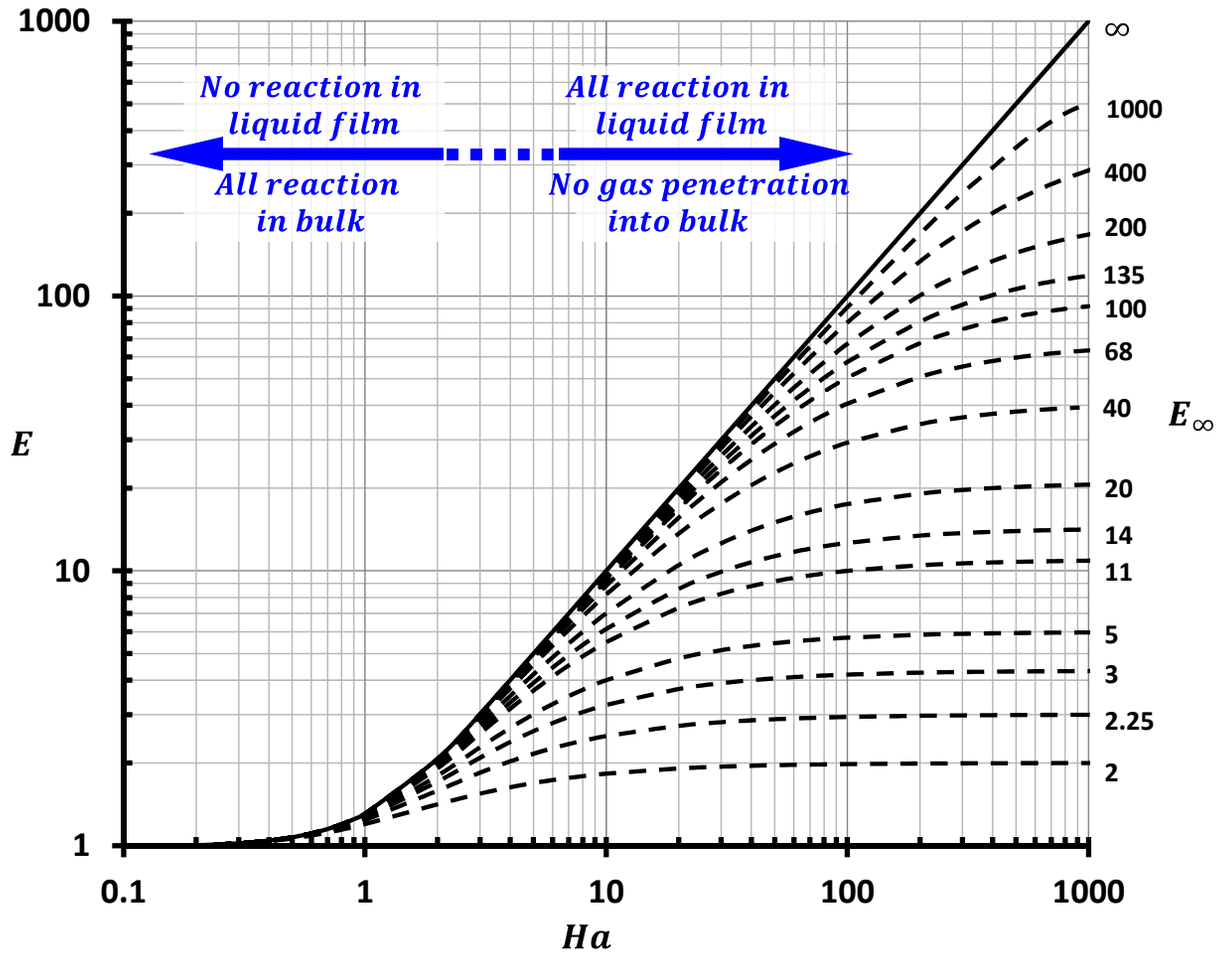


**Figure 5.** Enhancement factor for a first order gas-liquid reaction based on the numerical solution by van Krevelen and Hoftijzer [11]

### 3.2. Gas-solid systems

Gas-solid reactions are widely used in industrial applications. There are two main scenarios for gas-solid reactions, either the solid particles remain unchanged in size during reaction or they shrink with time as the reaction proceeds. The former scenario is described using the Continuous Reaction Model (CRM) as shown in Figure 6. This model assumes that the gaseous reactants react inside the solid particle, where its volume remains constant. On the other hand, the Shrinking Core Model (SCM), shown in Figure 7, assumes that the gas-phase reacts with the particle and the reaction front progressively moves inwards, continuously reducing the size of the core of unreacted solids and leaving behind reacted materials. The application of both of models were extensively discussed by Levenspiel [12].

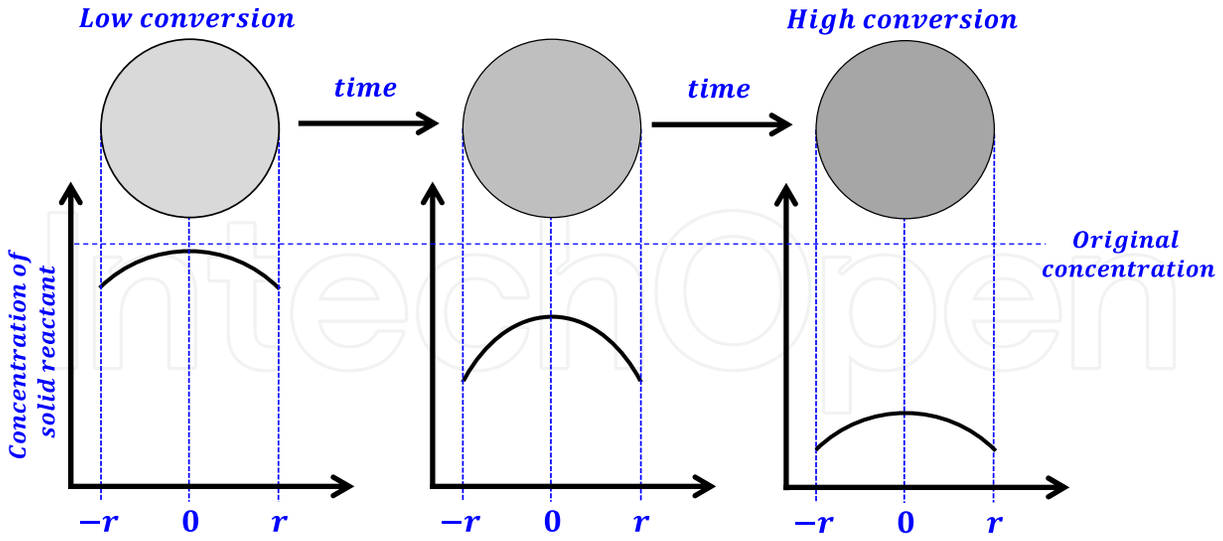


**Figure 6.** Schematic of the Continuous Reaction Model (CRM)

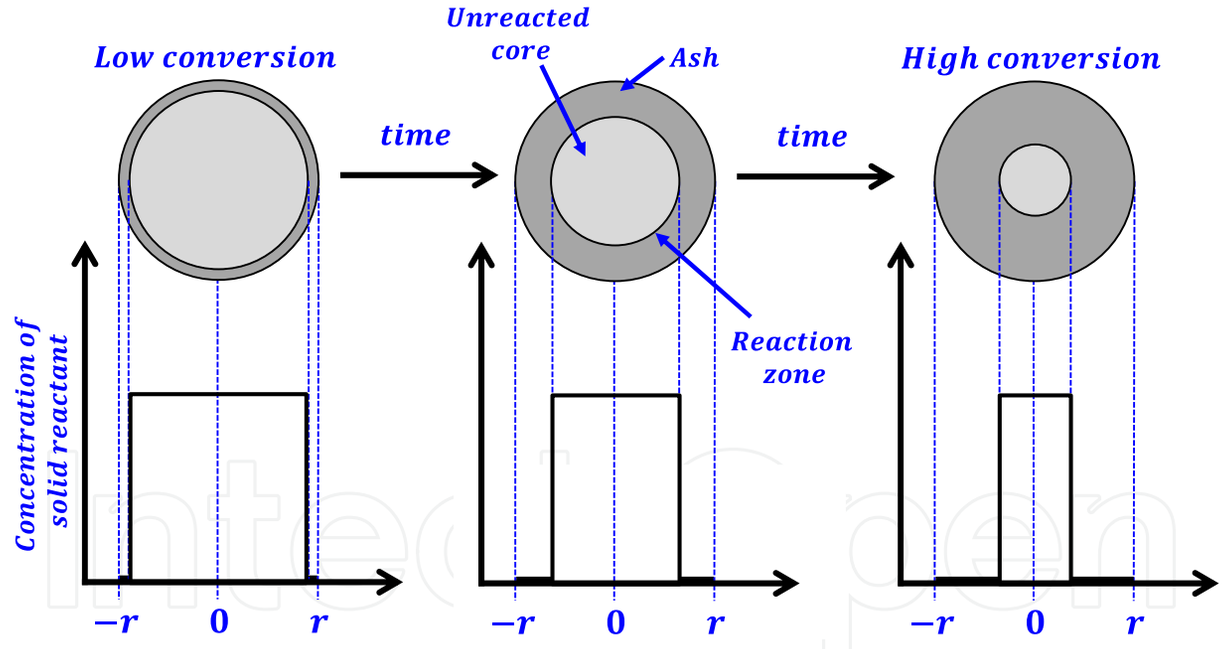


**Figure 7.** Schematic of the Shrinking Core Model (SCM)

### 3.3. Gas-liquid-solid systems

Figure 8 depicts a schematic of the concentration profile for mass transfer in three-phase systems, where the reactants in the gas-phase diffuse through the liquid-phase in order to reach the catalyst active sites to react, and then the products have to travel back to the gas-phase or to the liquid-phase. The following steps describe the mass transfer process:

1. Transfer of the reactants from the gas-phase bulk to the gas-side film.
2. Transfer of the reactants through the gas-side film to the gas-liquid interface
3. Transfer of the reactants form the gas-liquid interface through the liquid-side film.
4. Transfer of the reactants through the liquid bulk, then to the liquid film surrounding the catalyst particle.
5. Transfer of the reactants through liquid film surrounding the catalyst particles to the particle surface.
6. Diffusion of the reactants inside the particle pores to the catalyst active sites.
7. Reaction of the reactants to form products.
8. Diffusion of the products through the particle to its external surface.
9. Transfer of the products from the particle external surface through the liquid-film surrounding the particle.
10. Transfer of the products from the liquid-film surrounding the particle through the liquid bulk. Depending of the conditions, products could remain the liquid-phase.
11. Transfer of the gaseous products from the liquid bulk through the liquid-side film.
12. Transfer of the gaseous products from the liquid-side film to gas-liquid interface.
13. Transfer of the gaseous products from the gas-liquid interface to the gas-phase.

An example of processes where the products remain in the liquid phase is the synthesis of cyclohexanol and cyclohexanone by cyclohexane oxidation. These products remain in the liquid phase and their separation is achieved by simple distillation.

Steps 1-4 and 11-13 are evaluated considering the specific gas-liquid interfacial area ($a$) and the mass transfer coefficients in the gas-side film ($k_G$) and/or the liquid-side film ($k_L$). Steps 5 and 10 are accounted for through the particle specific surface area and solid-side mass transfer coefficient ($k_S$). Steps 6 and 8 are determined by the Knudsen diffusivity ($D_\kappa$) and the effective diffusion ($D_{eff}$) in the catalyst particle, using Equations (10) and (11) as:

$$D_\kappa = 97 r_p \sqrt{\frac{T}{M_L}} \tag{10}$$

$$D_{eff} = \varepsilon_{cat} \frac{D_{AB}}{\tau_{cat}} \tag{11}$$

Where $r_p$ represents the catalyst pore radius; $\varepsilon_{cat}$ is the catalyst void fraction; $\tau_{cat}$ is the tortuosity in the particle; and $M_L$ is the molecular weight of the liquid phase.

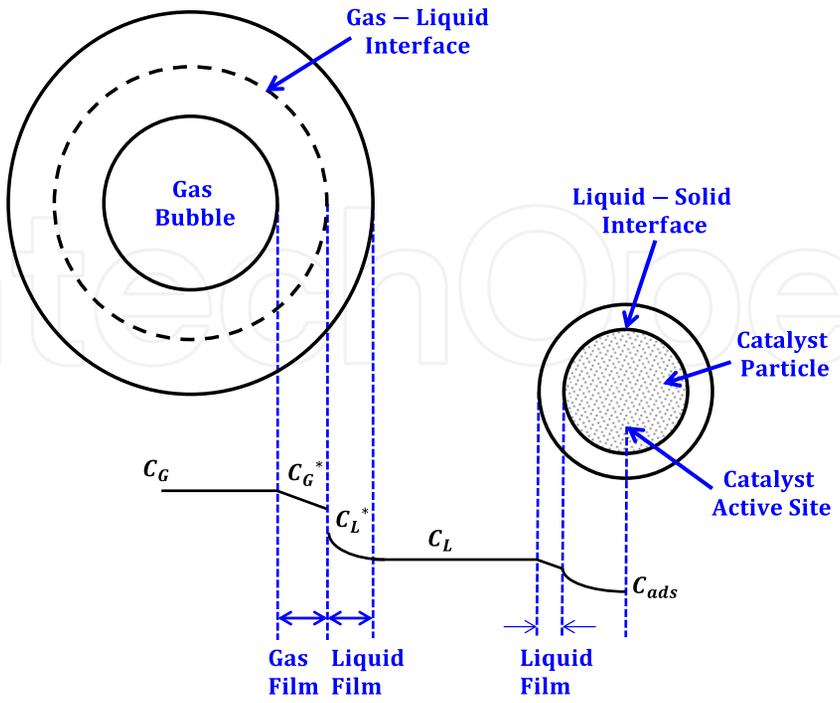


**Figure 8.** Concentration profiles for mass transfer into a slurry with a catalytic particles [13]

The reactions are quantified for the catalyst by the Thiele modulus ($\Phi_s$), which is valid for first order irreversible reaction, and the effectiveness factor ($\eta$), Equations (12) and (13).

$$\Phi_s = R_{cat}\sqrt{\frac{k_{reaction}}{D_{eff}}} \tag{12}$$

$$\eta = \frac{1}{\Phi_s}\left(\frac{1}{tanh\left(3\Phi_s\right)} - \frac{1}{3\Phi_s}\right) \tag{13}$$

Where $k_{reaction}$ is the reaction rate constant for a first order reaction, and *Rcat* is the particle radius. For particles smaller than 200 microns and having a small Thiele modulus, for all practical purposes, the effectiveness factor $\eta$ is close to unity.

Step 7 represents the chemical reaction of the reactants on the catalyst active sites. A typical first order reaction, which is usually found in hydrogenation processes, is:

$$r_i = A \cdot \eta \cdot exp\left(\frac{-E_{app}}{RT}\right) \cdot C_{L,H_2} \tag{14}$$

The effectiveness factor in this equation is obtained from Equation (13).

## 4. Measuring gas-liquid mass transfer in multiphase systems

Physical and chemical methods were used to measure the gas-liquid interfacial area ($a$) and mass transfer coefficients ($k_L$) in multiphase systems. The gas-liquid interfacial area was measured using different physical and chemical methods. Physical methods, including photography, light reflection and light scattering were used, however, they were restricted to transparent contactors having low gas holdup. Other physical methods, including $\gamma$–ray radiography and real time neutron radiography were also used to estimate $a$. While the aforementioned methods reveal the gas bubble contributions to $a$, other techniques were devised to determine the impact of gas-liquid interface ripple on $a$. For instance, Muenz and Marchello [14] measured the wave frequency using a stroboscope and determined the interface amplitude through analysis of the refractive surface properties via a photovolt photometer and densitometer. Moreover, Vazquez-Una et al. [15] used a CDD camera viewing the surface at a 45° angle to calculate through digitized images analysis the wavelength,$\lambda$. They determined the surface peak-to-peak amplitude and frequency from the surface displacement recorded using a vertically oriented laser triple-range distance-measuring device.

The chemical methods, on the other hand, were used to measure the gas-liquid interfacial area using a fast chemical reaction, where the reaction kinetics should be known in order to calculate $a$. Midoux and Charpentier [16] thoroughly reviewed various chemical reactions for measuring the gas-liquid interfacial area $a$.

Physical and chemical methods were also used to measure the volumetric mass transfer coefficient ($k_La$) since it was found that the liquid-side mass transfer coefficient ($k_L$) is strongly dependent on the turbulence induced in the multiphase systems. Among the physical methods is the transient physical gas absorption (TPGA) technique, which appears to be a simple and direct method for measuring $k_La$. For instance, Chang and Morsi [17] developed a powerful model to describe the transient pressure decline, based on a modified Peng-Robinson equation of state (EOS) and mass balance. In their method, the decline of the total pressure of the system with time was recorded, and in conjunction with total mole and volume balances, $k_La$ values were obtained under high pressures and temperatures for numerous gases (CO, $H_2$, $CH_4$, $CO_2$, $N_2$, He, etc.), into the liquids (hexane, toluene, cyclohexane, methanol, silicon oil, molten wax, polyalphaolefins, etc.) in the absence and presence of solids (glass beads, alumina, Puralox, iron oxides, etc.). The improvement brought by this model was discussed elsewhere [18]. The chemical methods for measuring $k_La$ were reviewed by Danckwerts et al. [5], Astarita [19] and Charpentier [20]. In these methods, a slow chemical reaction with known kinetics was employed to obtain $k_La$. The problems encountered in using these methods were due to the difficulty in controlling temperature and the lack of reliable kinetics.

The liquid-side mass transfer coefficient ($k_L$) could be indirectly calculated, knowing both the gas liquid interfacial area ($a$) and the volumetric mass transfer coefficient ($k_La$) determined using any of the physical methods described above. However, one must measure $k_La$ and $a$ simultaneously, i.e., under the same hydrodynamics in order to calculate a meaningful value of $k_L$. This is because as mentioned above $k_L$ strongly depends on the turbulence induced in the multiphase system. The liquid-side mass transfer coefficient ($k_L$) was also calculated using a

chemical reaction with known kinetics and a contactor with known surface area (gas-liquid interface). The knowledge of the total absorption rate, equilibrium solubility, and reaction kinetics would enable the calculation of $k_L$ [20]. Again, the difficulty in this method resides in the stability of the liquid film on the surface area of the contactor.

## 5. Literature data on gas-liquid mass transfer in multiphase systems

The effects of mass transfer on three-phase reactor performance have been extensively investigated in the literature. Earlier studies on the mass transfer in F-T systems focused on the significance of hydrogen mass transfer compared to the overall reaction resistance. This was due to the fact that F-T kinetics over iron catalyst were reported to be first order with respect to hydrogen. The principal mass transfer resistance occurs in the slurry-phase and the extent of the effect of gas-liquid mass transfer on the reactor performance has been argued. Satterfield and Huff [21] concluded that the hydrogen mass transfer was the limiting step for reactor productivity, whereas Deckwer [22] showed that the mass transfer resistance was smaller when compared with the kinetics resistance. Inga and Morsi [23] and Sehabiague and Morsi [24] reported that F-T SBCRs operating under a kinetically-controlled regime at low catalyst concentrations could move to a mass transfer-controlled regime at high catalyst concentrations, where the reactor performance quickly declines. Nonetheless, it is generally agreed that the mass transfer strongly depends on the bubble size, where smaller bubbles result in a greater gas-liquid interfacial area, which improves the overall mass transfer.

The volumetric mass transfer coefficients, derived from the inlet and outlet concentrations of absorption experiments, were influenced by the dispersion in both phases [13]. Since the dispersion is strongly dependent on the column size and geometry, the developed equations for the calculating the volumetric mass transfer coefficients appear to include geometric parameters, such as the column diameter and sparger characteristics. Behkish et al. [25, 26] measured the volumetric mass transfer coefficients ($k_La$) for $H_2$, CO, $N_2$, $CH_4$ and He in Isopar-M (an isoparaffinic liquid mixture of $C_{10} - C_{16}$) in the presence of alumina particles under high pressures (up to 30 bar), temperatures (up to 473 K), gas velocities (up to 0.39 m/s) and solid concentrations (up to 36 vol.%). While the experiments by these authors were conducted under typical F-T operating conditions, they did not use gas mixtures, mimicking the syngas; and the composition of their Isopar-M varies greatly from that of the molten wax produced in the SBCR once a steady-state operation is reached.

More recently, Sehabiague et al. [24] have measured the volumetric mass transfer coefficients for $N_2$ and He, in $C_{12}$-$C_{13}$, paraffins mixture, light F-T cut, heavy F-T cut in a 0.3 m ID SBCR under high pressures (up to 30 bar), temperatures (up to 500 K) in the presence of Alumina, Puralox Alumina and Iron oxide particles (up to 20 vol.%) at various superficial gas velocities (up to 0.27 m/s). Table 2 summarizes the literature studies and correlations for $k_La$ in multi-phase reactors over the past 20 years.

http://dx.doi.org/10.5772/60516

| System | Conditions | Correlation | Reference |
|---|---|---|---|
| Air, $N_2$ – Water, Alcohols, Calcium alginate, Polystyrene | $P_{atm}$<br>$u_g$ up to 0.15ms$^{-1}$<br>$C_V$ up to 20 vol%<br>$d_C$:0.14, 0.218, 0.3 m<br>$h_C$:1.5 m | $k_L a = \frac{12.9 Sc^{0.5} \varepsilon_g^{1.3}}{Mo^{0.159} Bo^{0.184}} \cdot \left(\frac{g \rho_l D_{AB}}{(1+0.62C_V)\cdot \sigma_l}\right)$<br>$\left(0.47 + 0.53\, exp\left(-41.4 \frac{\Pi_\infty k_l}{\mu_l u_p} Re_B^{-0.5}\right)\right)$<br>$\Pi_\infty = -C_B\left(\frac{d\sigma}{dC_B}\right)$ | Salvacion et al [27] |
| $O_2$, $CO_2$ – Glycol, Water, Brine, Aqueous Polyacrylamide | Sieve and Sintered plate | $k_L = \alpha\left(\frac{(\rho_l - \rho_g)\mu_l g}{\rho_l^2}\right)^{\frac{1}{3}}\left(\frac{\mu_l}{\rho_l D_{AB}}\right)^{-\frac{2}{3}}$<br>$\alpha = \begin{cases} 0.31 \;\; for \;\; d_p < 1.0 \;\; mm \\ 0.0031 \;\; for \;\; 1.0 < d_p < 2.5 \;\; mm \\ 0.0042 \;\; for \;\; d_p > 2.5 \;\; mm \end{cases}$ | Calderbank et al. [28] |
| $CO_2$ – $NaHCO_3$, $Na_2CO_3$ surfactants | $d_C$: 0.113 m , $h_C$: 1.086 m<br>$u_g$<0.002 ms$^{-1}$ | $k_L = K_4 u_g^{0.5} \sigma_l^{1.35}$<br>*$K_4$ is a function of the bubble plate size* | Vazquez et al. [29] |
| He, $N_2$, $SF_6$, Air – 0.8 M $Na_2SO_4$ - Xanthan gum, Diatomite, Alumina suspensions | P: 0.1 – 1 MPa<br>$u_G$:0.01−0.08 ms$^{-1}$<br>$C_V$ :Upto 18% vol<br>$d_p$:7, 22 μm<br>$d_C$:0.115 m , $h_C$:1.37 m | $k_L a = u_g^{0.9} \mu_{eff}^{-0.55} \rho_g^{0.46}$<br>$K = \begin{cases} 0.063 \;\; for \;\; Salt \;\; Solutions \\ 0.042 \;\; for \;\; Salt \;\; free \;\; Systems \end{cases}$<br>$\mu_{eff} = k(2800 u_g)^{n-1}$<br>*k is the fluid consistency index = 1.97 ,*<br>*n : empirical constant* $1 \geq n \geq 0.18$ | Dewes et al. [30] |
| $N_2$/Fe(CN) - NaOH, CMC,$HNaCO_3$-$Na_2CO_3$/glass, diatomite, silicon carbide, alumina | $u_g$: 0.007−0.09 ms$^{-1}$<br>$C_V$ : 1.3−12.4 vol%<br>$d_p$:44−105 μm<br>$\varrho_s$:2448−3965 kg/m$^3$<br>$\varrho_l$:1026−1121 kg/m$^3$<br>$\mu_l$:0.99−6.27 mPa · s<br>$d_C$:0.05 m , $h_C$:0.75 m | $\frac{k_L}{u_g} = 0.103(ReFrSc^2)^{-0.265}$ | Neme et al. [31] |
| Air - Water - Lexan, PS, Glass | $u_g$: 0.0025−0.05 ms$^{-1}$<br>$\varrho_s$:1170−2460 kg/m$^3$<br>$C_V$: 0.9−2.5 vol%<br>$d_p$:2.3−3 mm<br>$d_C$:0.06 m ,<br>$h_C/d_C$:22−30.2 | $k_L a = 4.49 u_g^{0.338} C_s^{0.595}\left(1 - \frac{\rho_l}{\rho_s}\right)^{0.337}$ | Guo et al. [32] |
| Air - Water - Nickel | $u_g$:0.02−0.04 m/s<br>$u_l$:0.018−0.037 m/s<br>$C_V$ : 5.7 vol.% | $k_L a = 0.4 u_g^{0.625} u_l^{0.26} \times exp[1.477 \cdot 10^{-5} h_C]$ | Chen et al. [33] |

| System | Conditions | Correlation | Reference |
|---|---|---|---|
| | $d_p$: 177−210 μm<br>$\varrho_s$: 8900 kg/m$^3$<br>$d_C$: 0.05 m ,<br>$h_C$: 0.5 m | | |
| $H_2$/CO - Paraffin oil - Silica gel | T: 293−523 K<br>P: 1−5 MPa<br>$d_p$: 134 μm<br>$C_v$: 5− 20 vol.%<br>$d_C$: 0.037 m , $h_C$: 0.48 m | $H_2$: $\frac{k_L\ d_{32}}{D_{AB}} = 1.546\times10^{-2} Eu^{0.052} Re^{0.076} Sc^{-0.231}$<br>$CO$: $\frac{k_L\ d_{32}}{D_{AB}} = 8.748\times10^{-2} Eu^{-0.012} Re^{0.024} Sc^{-0.133}$ | Yang et al. [34] |
| $H_2$, CO, $N_2$, $CH_4$- Isopar-M, Hexanes – Glass beads, Iron Oxide | $u_g$: 0.0035−0.574 m/s<br>$C_v$: 0 −36 vol.%<br>T: 275−538 K<br>P: 0.1−15 MPa<br>$\varrho_s$: 700−4000 kg/m$^3$<br>$d_p$: 5−300 μm<br>$\varrho_l$: 633.4−1583 kg/m$^3$<br>$\mu_l$: 0.189−398.8 mPa · s<br>$\sigma_l$: 8.4−75 mN/m<br>$d_C$: 0.0382−5.5 m | $\frac{k_L}{(1-\varepsilon_g)} = 6.14\times10^4 \cdot$<br>$\cdot \frac{\rho_l^{026}\mu_l^{0.12}\varepsilon_g^{1.21}D_{AB}^{0.5}}{\sigma_l^{0.52}\rho_g^{0.06}u_g^{0.12}d_p^{0.05}T^{0.68}}\Gamma^{0.11}\left(\frac{d_C}{d_C+1}\right)^{0.4}$ | Lemoine et al. [35] |
| $H_2$, CO, $N_2$, $CH_4$,-Isopar-M, Hexanes – Glass beads, Iron Oxide | Same as Lemoine et al. [35] | $k_L\ a = 0.18 Sc^{0.6}\left(\frac{\rho_l \eta_g}{M w_l}\right)^{-2.84}(\rho_g u_g)^{0.49}\times exp[-2.66C_V]$ | Behkish et al. [36] |
| He, $N_2$ – Paraffins mixture, $C_{12}$-$C_{13}$, Light F-T Cut, Heavy F-T- Cut – Alumina, Puralox Alumina, Iron oxide | $u_g$: 0.14−0.26 m/s<br>$C_v$: 0 −20 vol.%<br>T: 330−530 K<br>P: 8−30 MPa<br>$\varrho_s$: 3218−4000 kg/m$^3$<br>$d_p$: 1.5−140 μm<br>$\varrho_l$: 631.3−779.5 kg/m$^3$<br>$\mu_l$: 0.27−9.96 mPa · s<br>$\sigma_l$: 13−27 mN/m<br>$d_C$: 0.3 m m, $h_C$: 3 m | $k_L\ a = 7.99\times10^{-9}\frac{\rho_l^{1.82}\rho_g^{0.27}u_g^{0.387}\Gamma^{0.173}}{\mu_l^{0.25}\sigma_l^{0.976}M w_g^{0.02}}$<br>$\left(\frac{P_T}{P_T-P_S}\right)^{0.242}\left(\frac{d_C}{d_C+0.3}\right)^{0.1}\times exp$<br>$[-1.3C_v + 0.8C_v^2 - C_v^3 - 1675.7d_p + 0.176X_W]$ | Sehabiague et al. [24] |

**Table 2.** Recently published gas-liquid mass transfer empirical correlations applicable to multiphase reactors

http://dx.doi.org/10.5772/60516

## 6. Applications to Fischer-Tropsch synthesis

This Chapter focuses on the Fischer-Tropsch (F-T) synthesis process as an example of industrial multiphase systems. In this process, the syngas ($CO + H_2$) react in the presence of a catalyst, conventionally iron or cobalt, to produce synthetic hydrocarbon products, primarily linear alkanes and alkenes. The overall F-T process involves three main steps: syngas generation, F-T catalytic reactions and product upgrading. Syngas generation involves converting the carbonaceous feedstock into a $H_2$-CO mixture via reactions with steam and optionally oxygen or air. Solid feedstocks, such as coal and biomass, are converted in a gasifier, of which various types have been already in industrial applications [37-40]. Different gasification processes and technologies have also been discussed in the literature [41-52]. Natural gas, on the other hand, is converted to syngas in a reformer using either partial oxidation (POX), steam methane reforming (SMR) or auto-thermal reforming (ATR).

Although many metals have been identified to catalyze F-T reactions, only iron (Fe) and cobalt (Co) have been used in industrial applications [39, 52]. Iron catalyst is cheap and has a high water-gas-shift (WGS) activity, however, it is prone to severe attrition and the water produced during the reaction appeared to decrease its activity [53, 54]. Cobalt-based catalyst, on the other hand, has higher activity than iron catalyst since it is not strongly inhibited by water. It is more resistant to attrition and as such has a longer life in the reactor than iron catalyst. Cobalt-based catalyst, however, is more expensive and has no WGS activity [53, 55]. During Cobalt catalyzed F-T reaction, the oxygen from CO dissociation is converted to $H_2O$, as shown in Equation (15). Conversely, iron catalyst has a high affinity for the WGS reaction as shown in Equation (16), resulting in the conversion of a significant portion of oxygen from CO dissociation into $CO_2$.

$$F-T:\ CO+2H_2 \rightarrow -CH_2- +\ H_2O \tag{15}$$

$$WGS:\ CO+H_2O \leftrightarrows H_2+\ CO_2 \tag{16}$$

Thus, the extent of the WGS reaction has to be closely considered as it affects the $H_2$/CO ratio in the F-T process.

### 6.1. Multiphase Reactors for F-T synthesis

Depending on the reaction temperature, the F-T process is referred to as low temperature F-T (LTFT) or high temperature F-T (HTFT). The temperature of the LTFT ranges from 180 to 260 $^oC$ and the syncrude produced is wax consisting mostly of long chain hydrocarbons, while the temperature of the HTFT process is between 290 and 360 $^oC$ and the products are mostly short chain hydrocarbons and gases. Therefore, the final products of the LTFT process consist mostly of diesel fuel, while gasoline production has been the focus of the HTFT [56]. The LTFT syncrude product is easy to upgrade by a hydroprocessing step and a fractionation step to obtain naphtha and middle distillate, whereas the HTFT syncrude requires more complex

| F-T Plant | Date of Operation | Reactor Technology | Catalysts |
|---|---|---|---|
| German CTL (14 plants active at end of WWII) | 1935-1962 | LTFT FB | $Co/ThO_2$/kieselguhr (100:18:100) before 1938<br>$Co/ThO_2/MgO$/kieselguhr (100:5:8:200) after 1938 |
| Hydrocol GTL | 1951-1957 | HTFT FFB | Fused $Fe_3O_4/Al_2O_3/K_2O$ (97:2.5:0.5)<br>Later replaced by Magnetite with 0.5% $K_2O$ |
| Sasol I CTL/GTL | 1955-present | HTFT CFB<br>LTFT FB, SBCR | Magnetite with 0.5% $K_2O$<br>Precipitated $Fe/SiO_2/K_2O/Cu$ (100:25:5:5) |
| Sasol Synfuels CTL | 1980-present | HTFT FFB | Fused Fe (similar to Sasol I HTFT CFB catalyst) |
| PetroSA GTL | 1992-present | HTFT CFB<br>LTFT SBCR | Fused Fe (same as Sasol Synfuels)<br>Co based catalyst |
| Shell Bintulu | 1993-present | LTFT FB | $Co/Zr/SiO_2$ |
| Sasol Oryx GTL | 2007-present | LTFT SBCR | $Co/Pt/Al_2O_3$ |
| Shell Pearl GTL | 2011-present | LTFT FB | $Co/Zr/SiO_2$ |

**Table 3.** F-T Plants: catalysts and reactor technologies [53, 57]

refinery facilities [56]. It should be noted that recent R&D and commercial efforts have been focused on the LTFT due to the current drive for using more diesel engines than gasoline engines, the excellent quality of sulfur-free F-T diesel, and perhaps the mild conditions of the process.

Reactor technologies used for commercial applications of the F-T synthesis are summarized in Table 3. The HTFT reactors include fixed fluidized-bed reactors (FFBRs) and circulating fluidized-bed reactors (CFBRs), whereas multitubular fixed-bed reactors (FBRs) and slurry bubble column reactors (SBCRs) are used for the LTFT process. Also, LTFT micro-channel reactors for small-scale applications have been recently receiving considerable attention, even though no commercial applications are yet available.

In multi-tubular FBRs, the syngas flows through small diameter tubes packed with catalyst at small voidage, resulting in a high pressure drop and an increased operating cost. These reactors have comparatively complex heat transfer characteristics and their maximum production capacity is limited by the amount of heat which can be removed. Hot spots would ultimately result in carbon deposition on the catalyst surfaces and serious plugging of the reactor tubes. These types of reactors, however, have been used to carry out LTFT by Germany during WWII, Sasol since 1950's and Shell at the Bintulu GTL (Malaysia) and more recently at the Pearl GTL (Qatar) [41, 53, 57, 58].

SBCRs, on the other hand, have a simpler design and allow for much higher heat removal efficiencies than multitubular FBRs due to the presence of a large volume of the liquid-phase. Its advantages include a much greater flexibility than FBRs and its capital cost is 20 - 40% lower than that of multitubular FBRs [59]. However, the high mechanical shear on the catalyst, resulting in particles attrition and the lack of a reliable system for the fine particles separation from the liquid products, have delayed commercial deployment of SBCRs until the 1990's.

http://dx.doi.org/10.5772/60516

Conversely, microchannel reactors have a stationary catalyst bed combined with enhanced heat and mass transfer characteristics. Also, they are typically aimed at exploiting a different market than conventional reactors where their small size is an advantage. A schematic of both SBCR and FBR multiphase reactors is shown in Figure 9

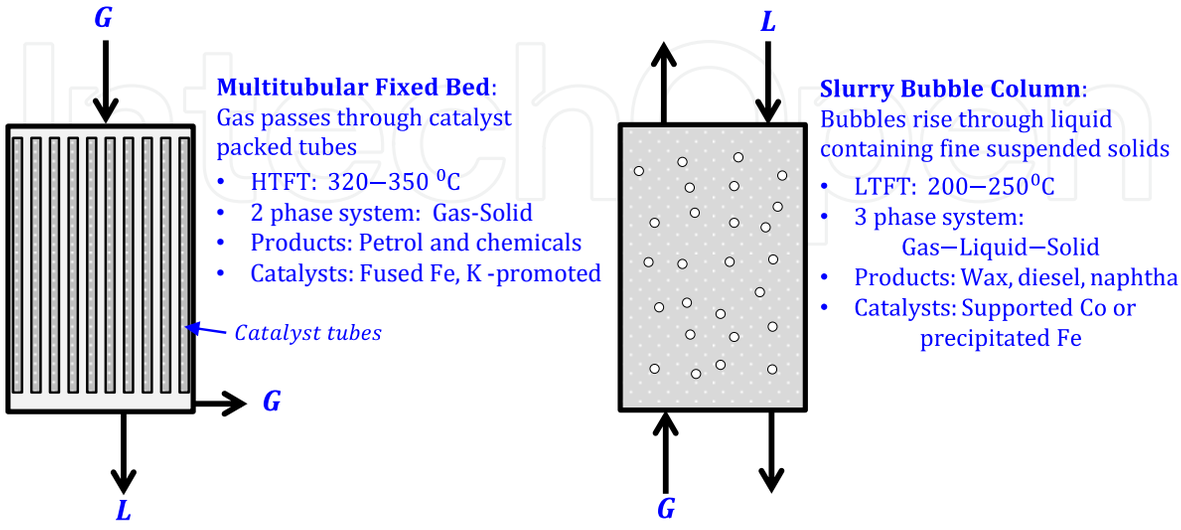


**Figure 9.** Schematic of SBCR and FBR reactors for F-T

### 6.2. Mass transfer in SBCRs for F-T synthesis

In general, the longer the molecules stay in the catalyst pores, the heavier the hydrocarbons become, significantly reducing their diffusivities, which could be considered as one of the main reasons for catalyst deactivation, referred to as fouling, in F-T synthesis [53]. In most applications, however, it is often assumed that when the products leave the solid-liquid interface, there is no major effect of their presence on the reaction rate. With these considerations, it can be concluded that the steps that affect the overall reaction rate of the process are the gas-liquid mass transfer step and the reaction on the catalyst active sites. This means that a major impact on the optimization of a gas-liquid or a gas-liquid-solid reactor could be done by increasing the catalyst activity and/or improving the mass transfer rate between the gas and the liquid phases. It should be mentioned, however, that the relative importance of the mass transfer, in certain processes depends on the catalyst activity, operating conditions, and reactor configuration [2].

Figure 8 shows the concentration profiles for mass transfer into a slurry system, and as such, it could be used to explain the mass transfer behavior in SBCRs. In F-T synthesis, since the diameter of catalyst particles used are in the range of 30 to 90 μm [60], the interfacial area between the liquid and the catalyst particles becomes very large and accordingly the resistance to the mass transfer due to steps 4, and 9 can be neglected. Steps 3 and 10 can also be neglected if the reactor is operated in the churn-turbulent flow regime due to the efficient mixing in this flow regime. Also, since the products formed in the F-T reactor are wax and as such the gas-phase consists mainly of the reactants (CO and $H_2$), one can neglect the resistance associated

with steps 1-2 and 13. Thus, the main resistances controlling the behavior of F-T synthesis in SBCRs are (1) the reaction kinetics (step 7), and (2) the gas-liquid mass transfer through the liquid-side film (steps 3 and 12).

## 7. Factors affecting the hydrodynamics and mass transfer in F-T SBCRs

The hydrodynamics (gas holdup, bubble size/distribution) and mass transfer characteristics (volumetric mass transfer coefficients) in SBCRs for F-T synthesis are affected by numerous factors ranging from the physicochemical properties of the gas-liquid-solid system to the operating conditions and reactor geometry. Unfortunately, the majority the experimental studies found in the literature on the hydrodynamics and mass transfer in SBCRs used air-water-glass beads systems under ambient conditions; and only few data are available under F-T conditions for $H_2$, CO, $N_2$ and He in F-T molten wax in the presence and absence of inert solid particles, including iron oxides, alumina and Puralox [24]. None of these studies, however, cover all the conditions encountered in an industrial F-T reactor ($T > 450$ K, $P > 20$ bar, $U_G > 0.15$ m/s, $C_V > 10$ vol%, mixture of hydrocarbons as liquid-phase, $H_2$ and CO as gas-phase, micron sized Fe or Co-based particles as solid-phase).

### 7.1. Effect of molecular weight and density of the gas-phase

The density of the gas-phase has been reported to increase the gas holdup [61, 62], and denser gases led to higher gas holdups. It was also reported that an increase of gas density resulted in the shrinkage of the gas bubbles [63]. The impact of the molecular weight of the gas phase is similar to that of the gas density. Indeed, an increase of the molecular weight will translate into an increase of gas density and as such will lead to higher gas holdup and smaller gas bubbles [64]. It is, however, important to note that the increase of gas holdup with density/molecular weight is not true under all conditions. Clark [65] for example reported that at low gas velocities below 0.05 m/s (corresponding to the homogeneous or bubbly flow regime), the gas holdup of $N_2$ was smaller than that of $H_2$.

### 7.2. Effect of density, viscosity and surface tension of the liquid phase

The effect of the liquid density on the gas holdup has been studied by several investigators, but still remains unclear. Some investigators reported an increase [66, 67] of gas holdup with increasing the liquid density, while others reported a decrease [62, 68]. The volumetric mass transfer coefficient was found to decrease with decreasing liquid density [69, 70]. Increasing the liquid viscosity has been found to decrease the gas holdup [61, 67, 68] and increase the gas bubbles size [71]. The volumetric mass transfer coefficient has been reported to decrease with increasing the liquid-phase viscosity [69, 70]. The liquid surface tension was reported to have a similar effect to that of the liquid viscosity on gas holdup, i.e., an increase of liquid surface tension leads to a decrease of gas holdup [61, 68]. Also, an increase of liquid surface tension leads to the formation of larger gas bubbles [71] and smaller volumetric mass transfer coefficients [69].

### 7.3. Effect of size, density and wettability of solid particles

Slurry suspensions of denser solid particles led to lower the gas holdup [72] than similar suspensions of particles with lower density. Increasing the size of solid particles was found to increase [72] the gas holdup for non-wettable solid particles, however, it was found to decrease [72, 73] the gas holdup for wettable solid particles. The solid particles diameter was reported, in some cases, to have no significant effect [74] on the gas holdup. The wettability of the solid particles has no clear effect on the gas holdup. In some cases, it was found to increase the gas holdup [72] and in others to decrease it [74].

### 7.4. Effect of operating conditions

Increasing temperature has been found to increase the gas holdup [36] through the decrease of both liquid surface tension and viscosity. Increasing temperature was also reported to increase the volumetric mass transfer coefficient [66] due in part to the increase of the gas diffusivity. On the other hand, the gas holdup was found to increase with pressure [75] which was attributed to the increase of the gas density. The volumetric mass transfer coefficient was also found to increase with pressure [75, 76]. Moreover, numerous experimental studies have shown that increasing the superficial gas velocity led to the increase of the gas holdup [62, 67] and the volumetric mass transfer coefficient [75, 76].

### 7.5. Effect of liquid and slurry velocity

The effect of liquid superficial velocity on the gas holdup has been investigated by several authors; and increasing liquid velocity was found to decrease the gas holdup in the absence [77] and presence [73, 74] of solid particles.

### 7.6. Effect of solid loading

The presence of fine micron-size catalyst particles in the liquid-phase greatly affects the properties of the slurry-phase, such as density and viscosity. While a few studies [24, 77] have found an increase of gas holdup with increasing solid concentration, adding more particles has mostly been found to decrease the gas holdup [63, 70, 73] by increasing the slurry viscosity. A decrease of the volumetric mass transfer coefficient and the formation of larger gas bubbles due to the increase of the rate of bubbles coalescence was also reported when increasing the solid loading [70]. It was also observed, particularly at low solid concentrations [78] that the volumetric mass transfer coefficient appeared to increase with increasing solid concentration. It should be noted that these results have to be considered along with the effects of the physical properties of the solids used, such as shape, size and wettability.

### 7.7. Effect of reactor geometry

The Reactor geometry has a strong influence on the gas holdup. In SBCRs, 3 zones can be identified where the gas holdups are significantly different. The first zone corresponds to the bottom of the reactor in the vicinity of the gas sparger, which is strongly affected by the sparger design. The second zone is the bulk region. The third zone is the top region, where the gas

holdup will behave very differently from the bulk region, if foaming occurs. It is important to note that if the reactor is long enough the effect of the first and third regions on the total gas holdup will become negligible [79]. The effect of column diameter on the gas holdup has been found to be strong in the case of small diameter reactors with diameter ≤ 0.15 m [80], however, several investigators have found that this effect would level off or disappear for diameters ≥ 0.15 m [69, 79]. Moreover, the length to diameter (L/D) ratio is frequently used instead of the reactor length when studying the effects of reactor geometry on the hydrodynamics. Several studies found that the gas holdup remained unaffected when the length to diameter ratio was ≥ 6 [24, 79].

### 7.8. Effect of gas distributor

The design of the gas distributor, the number of openings, their sizes and their orientations play an important role in affecting the hydrodynamics and mass transfer in the SBCRs not only within the bottom region at the vicinity of the gas distributor, but also in the bulk region. The initial bubble size and distribution at the orifice could be controlled by the sparger characteristics, but due to the balance between coalescence and breakup of gas bubbles, the initial bubble size created at the gas sparger would not describe the behavior of gas bubble size distribution in the entire column [71]. Under the same operating conditions, different designs of the gas sparger were found to give different volumetric mass transfer coefficient values [81]. For two different designs of the gas distributor, increasing the size of the openings was found to decrease gas holdup due to the formation of larger gas bubbles [36]. However, several investigators have reported that the gas sparger had a minimal effect on the bubble sizes and gas holdup if the orifice diameters were > 0.001-0.002 m [71, 79]. This suggests that for a certain size of the openings, the gas bubble size and gas holdup reach a maximum and a minimum value, respectively.

### 7.9. Effect of reactor internals

Since F-T synthesis is an exothermic reaction, cooling tubes are needed in the reactor in order to remove the heat released by the reaction. The presence of those internals will affect the performance of the reactor in terms of hydrodynamics and mass transfer. Saxena et al. [82] have studied 3 different configurations of internals representing 1.9%, 2.7% and 14.3% of the column cross sectional area and could not find any clear effect of the number of internals on the gas holdup. O'Dowd et al. [83] found slightly higher gas holdup value in a column equipped with cylindrical baffles occupying 15% of the cross-sectional area than in an unbaffled column of the same size. However, the difference lies within the range of errors of their experimental measuring technique. Also, another study [84] reported slightly higher gas holdup value when internals representing 5% of the cross section area were present. Yamashita [85] studied the effect of the separation distance between the internals and found out that gas holdup decreased when the separation distance was small (0.006 m) and increased when the separation distance was greater than 0.008 m. He attributed the decrease and increase in gas holdup values to the reduction of the radial mobility of gas bubbles and to the increase in interstitial gas velocity, respectively. Indeed, it is important to note that the slight increase in

http://dx.doi.org/10.5772/60516

gas holdup reported in the above mentioned studies might be the result of the increase of interstitial velocity inside the reactor when adding internals.

## 8. Concluding remarks

The knowledge of hydrodynamic and mass transfer parameters in multiphase systems is critical for the development of numerous industrial processes, and therefore proper understanding, measurement and quantification of these important parameters remains an area of significant interest from research and industrial perspectives. An important example of multiphase systems is the F-T synthesis and although interest in the design and scaleup of SBCRs for low temperature F-T has soared over the past two decades, there still remain significant knowledge gaps, which are yet to be investigated, particularly relating to investigation of the hydrodynamic and mas transfer parameters, such as gas holdup and $k_La$, under high pressures and temperatures typical to those of F-T industrial process. Such studies at elevated pressures and temperatures remain very limited when compared with the plethora of other studies conducted using air-water systems under ambient conditions. Thus, there is a great need for more studies to further understand the complex and intricate behavior of such multiphase systems and to investigate the effect of various operating parameters on the interphase mass transfer.

## Nomenclature

| | | | |
|---|---|---|---|
| $a$ | Interfacial area | $k_{reaction}$ | Reaction rate constant for a first order reaction (1/s) |
| Bo | Bond number | $k_L\ a$ | Volumetric liquid side mass transfer coefficient (1/s) |
| C* | Equilibrium concentration in the liquid phase ($mol \cdot m^{-3}$) | $M_L$ | Liquid average molecular weight ($kg \bullet kmol^{-1}$) |
| $C_L$ | Concentration in the liquid phase ($mol \cdot m^{-3}$) | P | Pressure (Pa) |
| Cv | Concentration of solid particles (vol.%) | r | Reaction rate ($mol \bullet kg^{-1}_{\ catalyst} \bullet s^{-1}$) |
| $d_c$ | Column diameter (m) | $r_p$ | Catalyst pore radius (m) |
| $d_p$ | Solid particle diameter (m) | Re | Reynolds number |
| $D_{AB}$ | Diffusivity of phase A into B | Mo | Morton number |
| $D_{eff}$ | Effective diffusivity in catalyst pores ($m^2 \cdot s^{-1}$) | s | Surface renewal frequency ($s^{-1}$) |
| $D_K$ | Knudsen diffusion ($m^2 \cdot s$) | Sc | Schmidt number |
| $E$ | Enhancement factor | t | Time (s) |

| | | | |
|---|---|---|---|
| Fr | Froude number | T | Temperature (K) |
| $g$ | Gravitational acceleration, (m/s$^2$) | $u_b$ | Gas bubble rise velocity (m·s$^{-1}$) |
| Ha | Hatta number | $u_g$ | Superficial gas velocity (m·s$^{-1}$) |
| $J_i$ | Molar flux of species i (kmol·s $^{-1}$·m$^{-2}$) | | |
| **Greek Letters** | | | |
| $\varepsilon_{cat}$ | Catalyst void fraction | $\pi$ | 3.14 |
| $\delta_L$ | Liquid film thickness (m) | $\rho$ | Density (kg/m$^3$) |
| $\eta$ | Effectiveness factor | $\sigma$ | Surface tension (N/m) |
| $\theta$ | Contact time | $\tau_{cat}$ | Tortuosity of the particle |
| $\mu$ | Viscosity (kg/m•s) | $\phi$ | Thiele modulus |
| **Subscripts** | | | |
| cat | Catalyst | l | Liquid |
| g | Gas | s | Solid |

## Author details

Badie I. Morsi* and Omar M. Basha

*Address all correspondence to: morsi@pitt.edu

Department of Chemical and Petroleum Engineering, University of Pittsburgh, Pittsburgh, PA, USA

## References

[1] A. Shanley, G. Parkinson, and K. Fouhy, "Biotech in the scaleup era," ed: McGraw Hill, 1993.

[2] J. R. Inga and B. I. Morsi, "A Novel Approach for the Assessment of the Rate-Limiting Step in Fischer-Tropsch Slurry Process," *Energy & Fuels,* vol. 10, pp. 566-572, 1996/01/01 1996.

[3] W. K. Lewis and W. G. Whitman, "Principles of Gas Absorption," *Industrial & Engineering Chemistry,* vol. 16, pp. 1215-1220, 1924.

[4] R. Higbie, "The rate of absorption of a pure gas into still liquid during short periods of exposure," *Transaction of the American Institute of Chemical Engineers,* vol. 31, pp. 365-389, 1935.

[5] P. V. Danckwerts, "Gas absorption accompanied by chemical reaction," *AIChE Journal,* vol. 1, pp. 456-463, 1955.

[6] K. Van't Riet, "Review of Measuring Methods and Results in Nonviscous Gas-Liquid Mass Transfer in Stirred Vessels," *Industrial & Engineering Chemistry Process Design and Development,* vol. 18, pp. 357-364, 1979/07/01 1979.

[7] J. T. Davies, A. A. Kilner, and G. A. Ratcliff, "The effect of diffusivities and surface films on rates of gas absorption," *Chemical Engineering Science,* vol. 19, pp. 583-590, 8// 1964.

[8] K. Kuthan and Z. Broz, "Mass transfer in liquid films during absorption Part III. Dependence of the liquid-side mass transfer coefficient on the molecular diffusivity of gases at high values of the schmidt number," *Chemical Engineering and Processing: Process Intensification,* vol. 25, pp. 75-84, 4// 1989.

[9] A. A. Kozinski and C. J. King, "The influence of diffusivity on liquid phase mass transfer to the free interface in a stirred vessel," *AIChE Journal,* vol. 12, pp. 109-116, 1966.

[10] V. Linek, J. Mayrhoferová, and J. Mošnerová, "The influence of diffusivity on liquid phase mass transfer in solutions of electrolytes," *Chemical Engineering Science,* vol. 25, pp. 1033-1045, // 1970.

[11] D. W. van Krevelen and P. J. Hoftijzer, "Kinetics of gas-liquid reactions part I. General theory," *Recueil des Travaux Chimiques des Pays-Bas,* vol. 67, pp. 563-586, 1948.

[12] O. Levenspiel, "Chemical reaction engineering," 1972.

[13] J. R. Inga, "Scaleup and Scaledown of Slurry Reactors: A New Methodology," ed, 1997.

[14] K. Muenz and J. M. Marchello, "Technique for Measuring Amplitudes of Small Surface Waves," *Review of Scientific Instruments,* vol. 35, pp. 953-957, 1964.

[15] G. Vázquez-Uña, F. Chenlo-Romero, M. Sánchez-Barral, and V. Pérez-Muñuzuri, "Mass transfer enhancement due to surface wave formation at a horizontal gas–liquid interface," *Chemical Engineering Science,* vol. 55, pp. 5851-5856, 12// 2000.

[16] J.-C. Charpentier, "Mass-Transfer Rates in Gas-Liquid Absorbers and Reactors," in *Advances in Chemical Engineering*. vol. Volume 11, G. R. C. J. W. H. Thomas B. Drew and V. Theodore, Eds., ed: Academic Press, 1981, pp. 1-133.

[17] M.-y. Chang and M. Badie I, "Mass transfer characteristics of gases in aqueous and organic liquids at elevated pressures and temperatures in agitated reactors," *Chemical Engineering Science,* vol. 46, pp. 2639-2650, // 1991.

[18] A. Behkish, "Hydrodynamic and Mass Transfer Parameters in Large-Scale Slurry Bubble Column Reactors," ed, 2004.

[19] G. Astarita, *Mass transfer with chemical reaction*: Elsevier, 1967.

[20] J. Charpentier, "Advances in chemical engineering," *Vol. II, Academic Press, New York,* 1981.

[21] G. A. Huff and C. N. Satterfield, "Intrinsic kinetics of the Fischer-Tropsch synthesis on a reduced fused-magnetite catalyst," *Industrial & Engineering Chemistry Process Design and Development,* vol. 23, pp. 696-705, 1984.

[22] W.-D. Deckwer, Y. Louisi, A. Zaidi, and M. Ralek, "Hydrodynamic Properties of the Fischer-Tropsch Slurry Process," *Industrial & Engineering Chemistry Process Design and Development,* vol. 19, pp. 699-708, 1980/10/01 1980.

[23] J. R. Inga and B. I. Morsi, "Effect of Operating Variables on the Gas Holdup in a Large-Scale Slurry Bubble Column Reactor Operating with an Organic Liquid Mixture," *Industrial & Engineering Chemistry Research,* vol. 38, pp. 928-937, 1999/03/01 1999.

[24] L. Sehabiague and B. I. Morsi, "Hydrodynamic and Mass Transfer Characteristics in a Large-Scale Slurry Bubble Column Reactor for Gas Mixtures in Actual Fischer–Tropsch Cuts," *International Journal of Chemical Reactor Engineering,* vol. 11, pp. 1-20, 2013.

[25] A. Behkish, R. Lemoine, L. Sehabiague, R. Oukaci, and B. I. Morsi, "Gas holdup and bubble size behavior in a large-scale slurry bubble column reactor operating with an organic liquid under elevated pressures and temperatures," *Chemical Engineering Journal,* vol. 128, pp. 69-84, 2007.

[26] A. Behkish, Z. Men, J. R. Inga, and B. I. Morsi, "Mass transfer characteristics in a large-scale slurry bubble column reactor with organic liquid mixtures," *Chemical Engineering Science,* vol. 57, pp. 3307-3324, 2002.

[27] J. Salvacion and M. Murayama, "Effects of alcohols on gas holdup and volumetric liquid-phase mass transfer coefficient in gel-particle-suspended bubble column.," *Journal of Chemical Engineering of Japan,* vol. 28, pp. 434-442, 1995.

[28] P. H. Calderbank and M. B. Moo-Young, "The continuous phase heat and mass transfer properties of dispersions," *Chemical Engineering Science,* vol. 50, pp. 3921-3934, 1995.

[29] G. Vázquez, E. Alvarez, J. M. Navaza, R. Rendo, and E. Romero, "Surface Tension of Binary Mixtures of Water + Monoethanolamine and Water + 2-Amino-2-methyl-1-propanol and Tertiary Mixtures of These Amines with Water from 25 °C to 50 °C," *Journal of Chemical & Engineering Data,* vol. 42, pp. 57-59, 1997/01/01 1997.

[30] I. Dewes and A. Schumpe, "Gas density effect on mass transfer in the slurry bubble column," *Chemical engineering science,* vol. 52, pp. 4105-4109, 1997.

[31] F. Neme, L. Coppola, and U. Böhm, "Gas holdup and mass transfer in solid suspended bubble columns in presence of structured packings," *Chemical Engineering & Technology,* vol. 20, pp. 297-303, 1997.

[32] Y. X. Guo, M. N. Rathor, and H. C. Ti, "Hydrodynamics and mass transfer studies in a novel external-loop airlift reactor," *Chemical Engineering Journal,* vol. 67, pp. 205-214, 1997.

[33] C.-M. Chen and L.-P. Leu, "Hydrodynamics and mass transfer in three-phase magnetic fluidized beds," *Powder Technology,* vol. 117, pp. 198-206, 2001.

[34] W. Yang, J. Wang, and Y. Jin, "Mass Transfer Characteristics of Syngas Components in Slurry System at Industrial Conditions," *Chemical Engineering & Technology,* vol. 24, pp. 651-657, 2001.

[35] R. Lemoine and B. I. Morsi, "Hydrodynamic and mass transfer parameters in agitated reactors part II: Gas-holdup, sauter mean bubble diameters, volumetric mass transfer coefficients, gas-liquid interfacial areas, and liquid-side mass transfer coefficients," *International Journal of Chemical Reactor Engineering,* vol. 3, p. 1166, 2005.

[36] A. Behkish, R. Lemoine, R. Oukaci, and B. I. Morsi, "Novel correlations for gas holdup in large-scale slurry bubble column reactors operating under elevated pressures and temperatures," *Chemical Engineering Journal,* vol. 115, pp. 157-171, 2006.

[37] K. Ripfel-Nitsche, H. Hofbauer, R. Rauch, M. Goritschnig, R. Koch, P. Lehner, *et al.*, "BTL–Biomass to liquid (Fischer Tropsch process at the biomass gasifier in Güssing)," in *Proceedings of the 15th European Biomass Conference & Exhibition, Berlin, Germany*, 2007.

[38] J. R. Longanbach, G. J. Stiegel, M. D. Rutkowski, T. L. Buchanan, M. G. Klett, and R. L. Schoff, "Capital and Operating Cost of Hydrogen Production from Coal Gasification," Final Report, U.S. DOE Contract No. DE-AM26-99FT40465, Subcontract No. 990700362, PittsburghApril 2003 2003.

[39] F. G. Botes, J. W. Niemantsverdriet, and J. van de Loosdrecht, "A comparison of cobalt and iron based slurry phase Fischer–Tropsch synthesis," *Catalysis Today,* vol. 215, pp. 112-120, 2013.

[40] A.-G. Collot, "Matching gasification technologies to coal properties," *International Journal of Coal Geology,* vol. 65, pp. 191-212, 2006.

[41] R. L. Espinoza, a. P. Steynberg, B. Jager, and a. C. Vosloo, "Low temperature Fischer–Tropsch synthesis from a Sasol perspective," *Applied Catalysis A: General,* vol. 186, pp. 13-26, 1999.

[42] A. Steynberg and M. Dry, *Fischer-Tropsch Technology*: Elsevier Science, 2004.

[43] M. Dry, "The fischer-tropsch process-commercial aspects," *Catalysis today,* vol. 9570, 1990.

[44] J. Xu and G. Froment, "Methane steam reforming, methanation and water-gas shift: I. Intrinsic kinetics," *AIChE Journal,* vol. 35, pp. 88-96, 1989.

[45] W. Mitchell, J. Thijssen, and J. M. Bentley, "Development of a Catalytic Partial Oxidation/Ethanol Reformer for Fuel Cell Applications," *Society of Automotive Engineers,* vol. Paper No.9, 1995.

[46] M. Bradford and M. Vannice, "Catalytic reforming of methane with carbon dioxide over nickel catalysts II. Reaction kinetics," *Applied Catalysis A: General,* vol. 142, pp. 97-122, 1996.

[47] K. Kusakabe, K.-I. Sotowa, T. Eda, and Y. Iwamoto, "Methane steam reforming over Ce–$ZrO_2$-supported noble metal catalysts at low temperature," *Fuel Processing Technology,* vol. 86, pp. 319-326, 2004.

[48] a. Berman, R. K. Karn, and M. Epstein, "Kinetics of steam reforming of methane on Ru/$Al_2O_3$ catalyst promoted with Mn oxides," *Applied Catalysis A: General,* vol. 282, pp. 73-83, 2005.

[49] P. Wu, X. Li, S. Ji, B. Lang, F. Habimana, and C. Li, "Steam reforming of methane to hydrogen over Ni-based metal monolith catalysts," *Catalysis Today,* vol. 146, pp. 82-86, 2009.

[50] A. J. de Abreu, A. F. Lucrédio, and E. M. Assaf, "Ni catalyst on mixed support of $CeO_2$–$ZrO_2$ and $Al_2O_3$: Effect of composition of $CeO_2$–$ZrO_2$ solid solution on the methane steam reforming reaction," *Fuel Processing Technology,* vol. 102, pp. 140-145, 2012.

[51] H.-S. Roh, I.-H. Eum, and D.-W. Jeong, "Low temperature steam reforming of methane over Ni–$Ce_{(1-x)}Zr_{(x)}O_2$ catalysts under severe conditions," *Renewable Energy,* vol. 42, pp. 212-216, 2012.

[52] D. A. Wood, C. Nwaoha, and B. F. Towler, "Gas-to-liquids (GTL): A review of an industry offering several routes for monetizing natural gas," *Journal of Natural Gas Science and Engineering,* vol. 9, pp. 196-208, 2012.

[53] M. E. Dry, "The Fischer-Tropsch process: 1950-2000," *Catalysis Today,* vol. 71, pp. 227-241, 2002.

[54] H. Schulz, G. Schaub, M. Claeys, and T. Riedel, "Transient initial kinetic regimes of Fischer–Tropsch synthesis," *Applied Catalysis A: General,* vol. 186, pp. 215-227, 1999.

[55] R. Deverell and M. Yu, "Long Run Commodity Prices: Where do we stand?," Credit Suisse27 July, 2011 2011.

[56] D. Leckel, "Diesel Production from Fischer−Tropsch: The Past, the Present, and New Concepts," *Energy & Fuels,* vol. 23, pp. 2342-2358, 2009/05/21 2009.

[57] A. de Klerk, *Fischer-Tropsch Refining*. Weinheim: Wiley-VCH Verlag & Co. KGaA, 2012.

[58] L. Sehabiague, "Modeling, Scaleup and Optimization of Slurry Bubble Column Reactors for Fischer-Tropsch Synthesis," Doctoral Dissertation, Department of Chemical and Petroleum Engineering, University of Pittsburgh, 2012.

[59] D. Gray, A. Elsawy, G. Tomlinson, G. J. Stiegel, and R. D. Srivastava, *Proceedings of the DOE Liquefaction Contractors' Review Meeting,* p. 344, 1991.

[60] A. Raje, J. R. Inga, and B. H. Davis, "Fischer-Tropsch synthesis: Process considerations based on performance of iron-based catalysts," *Fuel,* vol. 76, pp. 273-280, February 1997 1997.

[61] H. Hikita, S. Asai, K. Tanigawa, K. Segawa, and M. Kitao, "Gas hold-up in bubble columns," *The Chemical Engineering Journal,* vol. 20, pp. 59-67, 1980.

[62] I. G. Reilly, D. S. Scott, T. J. W. de Bruijn, and D. MacIntyre, "The Role of Gas Phase Momentum in Determining Gas Holdup and Hydrodynamic Flow Regimes in Bubble Column Operations," *Canadian Journal of Chemical Engineering,* vol. 72, pp. 3-13, 1994.

[63] A. Behkish, R. Lemoine, L. Sehabiague, R. Oukaci, and B. I. Morsi, "Gas holdup and bubble size behavior in a large-scale slurry bubble column reactor operating with an organic liquid under elevated pressures and temperatures," *Chemical Engineering Journal,* vol. 128, pp. 69-84, 1 April 2007 2007.

[64] P. M. Wilkinson and L. L. v. Dierendonck, "Pressure and gas density effects on bubble break-up and gas hold-up in bubble columns," *Chemical Engineering Science,* vol. 45, pp. 2309-2315, 1990.

[65] K. N. Clark, "The effect of high pressure and temperature on phase distributions in a bubble column," *Chemical Engineering Science,* vol. 45, pp. 2301-2307, 1990.

[66] U. Jordan, K. Terasaka, G. Kundu, and A. Schumpe, "Mass transfer in High-Pressure Bubble Columns with Organic Liquids," *Chemical Engineering & Technology,* vol. 25, pp. 262-265, 2002.

[67] T. Sauer and D.-C. Hempel, "Fluid dynamics and mass transfer in a bubble column with suspended particles," *Chemical Engineering & Technology,* vol. 10, pp. 180-189, 1987.

[68] L. S. Fan, G. Q. Yang, D. J. Lee, K. Tsuchiya, and X. Luo, "Some aspects of high-pressure phenomena of bubbles in liquids and liquid–solid suspensions " *Chemical Engineering Science,* vol. 54, pp. 4681-4709, 1999.

[69] K. Akita and F. Yoshida, "Gas Holdup and Volumetric Mass Transfer Coefficient in Bubble Columns. Effects of Liquid Properties," *Industrial & Engineering Chemistry Process Design and Development,* vol. 12, pp. 76-80, 1973/01/01 1973.

[70] K. Koide, A. Takazawa, M. Komura, and H. Matsunaga, "Gas holdup and volumetric liquid-phase mass transfer coefficient in solid-suspended bubble columns," *Journal of Chemical Engineering of Japan,* vol. 17, pp. 459-466, 1984.

[71] K. Akita and F. Yoshida, "Bubble size, Interfacial Area, and Liquid-Phase Mass Transfer Coefficient in Bubble Columns," *Industrial & Engineering Chemistry Process Design and Development,* vol. 13, pp. 84-91, 1974.

[72] M. Jamialahmadi and H. Müller-Steinhagen, "Effect of Solid Particles on Gas Hold-Up in Bubble Columns," *Canadian Journal of Chemical Engineering,* vol. 69, pp. 390-393, 1991.

[73] S. Kara, B. G. Kelkar, Y. T. Shah, and N. L. Carr, "Hydrodynamics and axial mixing in a three-phase bubble column," *Industrial & Engineering Chemistry Process Design and Development,* vol. 21, pp. 584-594, 1982/10/01 1982.

[74] B. G. Kelkar, Y. T. Shah, and N. L. Carr, "Hydrodynamics and axial mixing in a three-phase bubble column. Effects of slurry properties," *Industrial & Engineering Chemistry Process Design and Development,* vol. 23, pp. 308-313, 1984.

[75] H. Kojima, J. Sawai, and H. Suzuki, "Effect of pressure on volumetric mass transfer coefficient and gas holdup in bubble column," *Chemical Engineering Science,* vol. 52, pp. 4111-4116, 1997.

[76] A. Behkish, Z. Men, J. R. Inga, and B. I. Morsi, "Mass transfer characteristics in a large-scale slurry bubble column reactor with organic liquid mixtures," *Chemical Engineering Science,* vol. 57, pp. 3307-3324., 2002.

[77] D. B. Bukur, S. A. Patel, and J. G. Daly, "Gas holdup and solids dispersion in a three-phase slurry bubble column," *AIChE Journal,* vol. 36, pp. 1731-1735, 1990.

[78] A. Schumpe, A. K. Saxena, and L. K. Fang, "Gas/liquid mass transfer in a slurry bubble column," *Chemical Engineering Science,* vol. 42, pp. 1787-1796, 1987.

[79] P. M. Wilkinson, A. P. Spek, and L. L. van Dierendonck, "Design Parameters Estimation for Scale-up of High-Pressure Bubble Columns," *AIChE Journal,* vol. 38, pp. 544-554, 1992.

[80] F. Yoshida and K. Akita, "Performance of Gas Bubble Columns: Volumetric Liquid-Phase Mass Transfer Coefficient and Gas Holdup," *AIChE Journal,* vol. 11, pp. 9-13, 1965.

[81] U. Jordan and A. Schumpe, "The gas density Effect on Mass Transfer in Bubble Columns with Organic Liquids," *Chemical Engineering Science,* vol. 56, pp. 6267-6272, 2001.

[82] S. C. Saxena, N. S. Rao, and P. R. Thimmapuram, "Gas Phase Holdup in Slurry Bubble Column for Two- and Three-Phase Systems," *The Chemical Engineering Journal,* vol. 49, pp. 151-159, 1992.

[83] W. O'Dowd, D. N. Smith, J. A. Ruether, and S. C. Saxena, "Gas and solids behavior in a baffled and unbaffled slurry bubble column," *AIChE Journal,* vol. 33, pp. 1959-1970, 1987.

[84] J. Chen, F. Li, S. Degaleesan, P. Gupta, M. H. Al-Dahhan, M. P. Dudukovic*, et al.*, "Fluid dynamic parameters in bubble columns with internals," *Chemical Engineering Science,* vol. 54, pp. 2187-2197, 1999.

[85] F. Yamashita, "Effects of Vertical Pipe and Rod Internals on Gas Holdup in Bubble Columns," Journal of Chemical Engineering of Japan, vol. 20, pp. 204-206, 1987.

IntechOpen